



TECHNICAL UNIVERSITY OF CLUJ-NAPOCA

ACTA TECHNICA NAPOCENSIS

Series: Applied Mathematics, Mechanics, and Engineering

Vol. 66, Issue III, August, 2023

STUDY ON THE PRE-DESIGN OF AN OFFSHORE MONOPILE WIND TURBINE INSTALLED IN ROMANIAN SECTOR OF THE BLACK SEA

Mariea MARCU

Abstract: The paper shows the general characteristics of an offshore wind turbine and also a study of the environmental loads acting on its support. As it appears from many studies published in recent years, the western Black Sea is suitable for the installation of an efficient wind farm. We chose a monopile substructure as this is suitable for the water depth in that area. Based on environmental data from the Romanian sector of the Black Sea, we study how the environmental characteristics and the size of the monopile influence the total force and total bending moment acting on the structure. In this way, we identified the worst-case scenario and analyzed the dimensions of the monopile to propose a preliminary design.

Keywords: offshore wind turbine, monopile, wave, and wind load, bending moment, pre-design, Black Sea

1. INTRODUCTION

Offshore wind turbines are more and more used on the onshore and offshore areas in many regions of the globe. As it results from the Annual Wind Report 2022 [8] the offshore wind turbines in the entire world provided 22.3% of total wind energy. In 2022 Romania installed onshore a wind power capacity of 3.015 GW [19]. To install the wind farm in offshore areas, many studies have been elaborated [13][14] to identify the appropriate conditions in the Black Sea. These studies are focused on the evaluation of the wind and wave power potential in different areas of the Black Sea. None of these addressed the environmental loads which act on the offshore support of a wind turbine. Therefore, in this paper, our aim is to pre-design a monopile and study the wave and wind loads which act on that.

2. WIND TURBINE

A wind turbine first converts wind energy into mechanical energy which in turn activates a generator that produces electricity.

The wind turbine is an old concept adapted to the new green energy requests. Over time, many types of wind turbines have been proposed. Some of these had blades, others didn't. Also, the axis of the turbines can be horizontal or vertical.

From the multitude of turbine types, some have proven to be more efficient than others being used on a large scale. The most used types of wind turbines are those with three blades and a horizontal axis [7]. These are reliable because they have a low variation of torque during the motor shaft rotation [25].

The main components of the three blades and horizontal axis wind turbine (fig.1) are [24][7]:

- Rotor with three blades and the hub which connects the blades;
- Nacelle where are installed the generator, the gearbox, and the mechanical brake. The gearbox converts the speed rotation of the rotor to the speed rotation of the generator. The mechanical brake is used to stop the rotor when it is necessary like during maintenance, during extreme winds, etc.
- Pivoting system for turning the nacelle into the wind direction.
- Tubular steel tower (the most used) has different diameters and wall thicknesses

along its height. This supports the rotor and nacelle.

- Foundation with different configurations, which must resist to axial and lateral loads and to ensure lateral stability(fig.2).

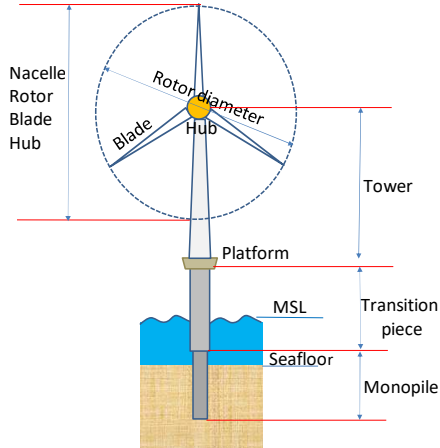


Fig.1. The main components of an offshore wind turbine.

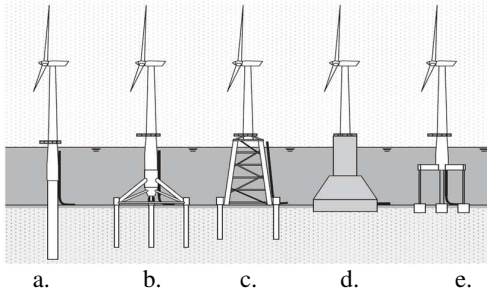


Fig.2. Different types of foundations for offshore wind turbines: a. monopile, b. tripod, c. jacket, d. gravity base, e. floating [17].

Fig.1 shows a monopile offshore wind turbine. In this case, the foundation consists of a monopile that is partially driven into the seafloor and a transition piece between the monopile and the wind turbine tower. The monopile can be driven into the seafloor with hydraulic hammers or inserted into a pre-drilled borehole in the hard seafloor rock.

The transition piece supports the auxiliary structures (boat landing, J-tubes, and platform). This piece can be missing when the pile is inserted into a pre-drilled hole. In this case, the monopile supports the auxiliary structures [17].

The substructures can have different configurations depending on the water depth(fig.2).

These substructures can be fixed or floating [4]. Those fixed can be monopile, tripod, jacket,

and gravity base and can be used in relatively shallow waters [4][17].

Compared with an onshore wind turbine, the offshore wind turbine is more affected by environmental loads. Therefore, the wind acts on the tower and at the hub level, and waves and currents act on the substructure. In addition to these loads, the turbine itself induces specific loads during its operation caused by the rotor vibration at the hub level and the and blade shadowing effect [6].

In the next section, we will study the environmentally induced loads (generated by wind and waves) that act on a monopile.

3. WAVE LOADS

To estimate the wave loads which act on the slender monopile we use Airy's linear waves theory and Morrison equation which are appropriate for preliminary design [18].

The water depth is categorized by the value of kd product as follows[3]:

- Deep for $kd > \pi$ or $d/L > 0.5$
- Intermediate for $0.1\pi < kd < \pi$ or $0.05 < d/L < 0.5$
- Shallow for $kd < 0.1\pi$ or $d/L \leq 0.05$

where L is the wavelength, d is water depth and k is wave number ($k = 2\pi/L$).

From the Airy linear wave theory, we determine the variation of the free surface elevation, $\eta(x, t)$, and the horizontal components of velocity, $u(x, t)$, and acceleration, $\dot{u}(x, t)$ of the water particles. These are determined along the wave at a level z between the mean sea level(MSL) and the water depth, d , with the following equations:

$$\eta(x, t) = a \cdot \cos(kx - \omega t) \quad (1)$$

$$u(x, t) = \frac{a\omega \cdot \cosh(k(z+d))}{\sinh(kd)} \cdot \cos(kx - \omega t) \quad (2)$$

$$\dot{u}(x, t) = \frac{\partial u(x, t)}{\partial t} = \frac{a\omega^2 \cdot \cosh(k(z+d))}{\sinh(kd)} \cdot \sin(kx - \omega t) \quad (3)$$

where, a is the wave amplitude, m;

ω – wave angular frequency, $\omega = 2\pi/T$, rad/s;

t –time, s;

T – wave period, s;
 H – wave height, $H = 2a$, m;
 x, z – horizontal and vertical coordinate axes;
 $x = 0$ at the origin of the axis; $z = 0$ at mean water level, $z = -d$ at the seafloor and $z = \eta(x, t)$ at the instant water free surface elevation. The wave number, k , is related to the angular wave frequency, ω , by the dispersion relationship:

$$\omega^2 = gk \tanh(kd) \quad (4)$$

or

$$\frac{2\pi}{T^2} = \frac{g}{L} \tanh\left(\frac{2\pi d}{L}\right) \quad (5)$$

When the equations above are satisfied, the free propagation of linear gravity waves with an amplitude, of a is produced [3]. The wavelength, L , is calculated from the dispersion equation (5).

Equations (2) and (3) depend on the values of kd product that are different for deep, intermediate, and shallow water. These equations correspond to the intermediate water conditions. In the case of deep water, the limit is $kd = \pi$ and $\tanh(\pi) \approx 1$. Therefore, some simplifications can be made, and the equations (2) and (3) become:

$$u(x, t) = a\omega e^{kz} \cdot \cos(kx - \omega t) = \frac{\pi H}{T} \cdot e^{kz} \cos(kx - \omega t) \quad (6)$$

$$\dot{u}(x, t) = a\omega^2 e^{kz} \cdot \sin(kx - \omega t) = \frac{2\pi^2 H}{T^2} e^{kz} \sin(kx - \omega t) \quad (7)$$

In figure 3 we show the linear wave model parameters according to Airy's wave theory.

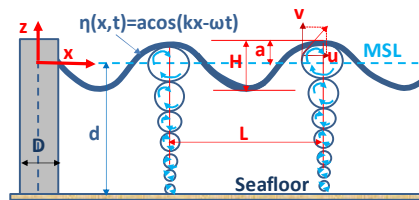


Fig. 3. Airy's linear wave model.

On the basis of the water particles' velocity and acceleration equations, we can determine the force of waves parallel to the flow direction which acts on the monopile immersed in seawater. The monopile model is a vertical

cylinder extending above the water level and embedded in the seafloor. In this case, we use the equation of Morison which has two components, namely the drag load component and the inertia load component.

Therefore, according to Morison, the wave force, $dF(z, t)$, per unit height of a vertical cylinder with diameter, D is:

$$dF(z, t) = dF_i(t) + dF_D(t) = \left(\frac{\pi}{4}\right)C_M\rho D^2 \cdot \dot{u}(z, t) + 0.5C_D\rho D \cdot u(z, t)|u(z, t)| \quad (8)$$

where $F_i(t)$ and $F_D(t)$ are inertia and drag force, N;

C_M and C_D – inertia and drag coefficients;

ρ – sea water density, kg/m^3 ;

$u(z, t)$ – horizontal velocity of water particles, m/s;

D – vertical cylinder diameter, m.

The inertia and drag coefficients depend on the Keulegan-Carpenter number, KC , the cylinder roughness, and the Reynold number. The Keulegan-Carpenter number shows the relative contribution of the inertia and drag forces in the total force and is defined by the following equation [3]:

$$KC = \frac{u_{max}T}{D} \quad (9)$$

The drag coefficient, C_D , and inertia coefficient, C_M values[3] are $C_D \in [0.6; 1.6]$ and $C_M \in [1.5; 2.15]$.

The total wave force acting on the height of a cylinder, results from the integration of the equation (8) between the seafloor where $z = -d$ and surface water elevation, where $z = \eta(x, t)$ as follows:

$$F(t) = \int_{-d}^{\eta} dF(z, t) dz = \frac{\pi}{4} C_M \rho D^2 \int_{-d}^{\eta} \dot{u}(z, t) dz + \frac{1}{2} C_D \rho D \int_{-d}^{\eta} u(z, t) |u(z, t)| dz \quad (10)$$

Vugts et. al[18] considered the integration of the force $dF(z, t)$ between $z = -d$ and mean sea level ($z = 0$). They show that simplification will affect only the drag force when this is dominant.

If we insert equations (2) and (3) into equation (10) and integrate it, we get the total wave force $F(t)$ for intermediate water depth as follows:

$$F(t) = F_i(t) + F_D(t) = \frac{\pi^3 H}{2kT^2} C_M \rho D^2 \sin(kx - \omega t) + \frac{1}{8k} C_D \rho D \left(\frac{\pi H}{T} \right)^2 \frac{\sinh(2kd) + 2kd}{(\sinh(kd))^2} \cos(kx - \omega t) | \cos(kx - \omega t) | \quad (11)$$

If we consider $x = 0$, the maximum of the inertia force is obtained when $\sin(-\omega t) = -\sin\left(\frac{2\pi}{T}t\right) = -1$, i.e. when $t = 3T/4$ and $\eta(t) = 0$.

The maximum of the drag force is obtained when $\cos(kx - \omega t) = 1$, i.e. when $t = 0$ and $\eta(t) = H/2$. As we observe, the inertia force and drag force have the maximum values at different times. Therefore, the maximum inertia force and maximum drag force for intermediate water depth, according to Vugts et al.[18], have the following expressions:

$$F_{I_{max}} = \rho g \cdot \frac{C_M \pi D^2}{4} a \cdot \tanh(kd) \quad (12)$$

$$F_{D_{max}} = \rho g \cdot \frac{C_D D}{2} a^2 \cdot \left(\frac{1}{2} + \frac{kd}{\sinh(2kd)} \right) \quad (13)$$

Arrany et al. [11] considered the integration of the equation (10) between $z = -d$ and instant water elevation $z = \eta(x, t)$, and they determined the maximum of the inertia and drag forces. Taking into account the conditions under which the maximum values of the forces are obtained, as well as the dispersion equation (4), the relations of Arrany et al. [1] become:

$$F_{I_{max}} = \rho g a \frac{C_M \pi D^2}{4} \tanh(kd) \quad (14)$$

$$F_{D_{max}} = \rho g a^2 \frac{C_D D}{4} \left(\frac{\sinh(2k(d+a)) + 2k(d+a)}{\sinh(2kd)} \right) \quad (15)$$

If we look at equations (12) and (14) we notice that they are identical, which means that the integration limits do not affect the maximum of the inertia force because it occurs at $\eta = 0$.

Alternatively, the drag force is affected by these limits because its maximum occurs at the $\eta = H/2 = a$. The bending moment at the mudline level is determined taking into account the force $F(t)$ and the distance between the seafloor and the water level. Therefore, the bending moment of the waves forces on the monopile is:

$$M(t) = \int_{-d}^{\eta} dF(z, t)(d+z)dz \quad (16)$$

The maximum bending moments generated by the inertia force, $M_{I_{max}}$ and by the drag force, $M_{D_{max}}$ according to Vugts et al[18] are:

$$M_{I_{max}} = \rho g a d \frac{C_M \pi D^2}{4} \left[\tanh(kd) + \frac{1}{kd} \left(\frac{1}{\cosh(kd)} - 1 \right) \right] \quad (17)$$

$$M_{D_{max}} = \rho g \cdot \frac{C_D D}{2} a^2 \left[\frac{d}{2} + \frac{2(kd)^2 + 1 - \cosh(2kd)}{4k \sinh(2kd)} \right] \quad (18)$$

If we consider the relations proposed by Arrany et al[1] and the dispersion equation(4) the maximum bending moments given by the inertia force, $M_{I_{max}}$ and drag force, $M_{D_{max}}$ are:

$$M_{I_{max}} = \rho g a \frac{C_M \pi D^2}{4k \cosh(kd)} \cdot [k(d+a) \sinh(k(d+a)) - \cosh(k(d+a)) + 1] \quad (19)$$

$$M_{D_{max}} = \rho g D \frac{C_D a^2}{16k \cdot \cosh(kd)} \cdot [2k(d+a) \sinh(2k(d+a)) - \cosh(2k(d+a)) + 2k^2(d+a)^2 + 1] \quad (20)$$

Therefore, the total wave force, $F_{T_{max \text{ wave}}}$ and total wave bending moment, $M_{T_{max \text{ wave}}}$ are:

$$F_{T_{max \text{ wave}}} = F_{I_{max}} + F_{D_{max}} \quad (21)$$

$$M_{T_{max \text{ wave}}} = M_{I_{max}} + M_{D_{max}} \quad (22)$$

4. WIND LOADS

Wind speed has a static component defined by the mean wind speed and a dynamic

component defined by the turbulent wind speed. Therefore, wind speed, U is $U = \bar{U} + u_{ext}$.

The wind speed is usually reported at 10 m above sea level. To extrapolate it at the hub level, we use the following relation:

$$U_{z\text{ hub}} = U_{z=10\text{m}} \frac{\ln(z_{\text{hub}}/z_0)}{\ln(z_{h=10\text{m}}/z_0)} \quad (23)$$

A wind turbine operates in a certain wind speed range between the cut-in and cut-out speed, which is generally between 4 m/s and 24 m/s. At cut-out speed the turbine is shut-down.

The wind speed is not constant; it changes rapidly even within seconds. This is called a gust that has an average speed in an interval of 10 minutes. The gust can return every year or every 50 years.

The DNV code [19] suggests the analysis of several extreme scenarios. Of these, Arany et al. [1] consider that the most important wind load occurs when an extreme 50-year gust hits the rotor at the rated speed.

The relation to determine the wind force which acts on the rotor, or thrust force is the following [1][6]:

$$F_{\text{wind}} = \frac{1}{2} \rho_{\text{air}} A_R C_T (U_R + u_{ext})^2 \quad (24)$$

where ρ_{air} is air density, $\rho_{\text{air}} = 1.225 \text{ kg/m}^3$
 A_R – turbine rotor area, m^2 ;

C_T – thrust coefficient;

U_R – rated wind speed, m/s;

u_{ext} – extreme gust, m/s.

According to the references[1][6][19], extreme gust, u_{ext} can be determined with the following equation:

$$u_{ext} = \min \left\{ 1.35(U_{10,1\text{-year}} - U_R); \right. \\ \left. 3.3\sigma_{U,c}/(0.1D_R/\Lambda_1) \right\} \quad (25)$$

$U_{10,1\text{-year}}$ – 10 minutes' wind speed with 1-year return period, m/s;

Λ_1 –longitudinal turbulence scale parameter, m

$\Lambda_1 = L_k/8.1$; $L_k = 340.2 \text{ m}$;

L_k –standard integral length scale, m;

D_R – turbine rotor diameter, m;

$\sigma_{U,c}$ – the characteristic standard deviation of wind speed, m/s.

$$\sigma_{U,c} = 0.11U_{10,1\text{-year}} \quad (26)$$

The 10 min wind speed with 1-year return can be determined as follows:

$$U_{10,1\text{-year}} = 0.8U_{10,50\text{-year}} \quad (27)$$

In the relation (27), $U_{10,50\text{-year}}$ is the 10 min wind speed with a 50-year return in m/s determined as follows:

$$U_{10,50\text{-year}} = k[-\ln(1 - 0.98^{1/52596})]^{1/s} \quad (28)$$

where k and s are parameters of wind speed Weibull distribution which can be estimated as follows [16]:

$$s = \frac{\sigma_U}{\bar{U}} \quad (29)$$

$$k = \bar{U}(0.568 + 0.433/s)^{-1/s} \quad (30)$$

where \bar{U} means wind speed in m/s, and σ_U is the standard deviation of wind speed, m/s.

The thrust coefficient must have values less than unity [1] and can be calculated for the wind speed range between cut-in speed and rated wind speed with the Frohboese-Schmuck[5] equation:

$$C_T = 3.5(2U_R + 3.5)/U_R^2 \quad (31)$$

Once determined the thrust force, the wind bending moment, M_{wind} can be determined as follows:

$$M_{\text{wind}} = F_{\text{wind}}(d + z_{\text{hub}}) \quad (32)$$

The DNV and IEC codes [20][21][22] recommended applying a load factor, $\gamma_L = 1.35$ to the wind bending moment calculated values. Then the total wind bending moment is:

$$M_{T\text{wind}} = 1.35M_{\text{wind}} \quad (33)$$

5. WAVE AND WIND LOADS

In our work, we consider only the wave and wind forces acting on the wind turbine structure because these forces are the most important [1][6]. Therefore, the total wave and wind force and bending moment are as follows:

$$F = F_{Tmax\ wave} + F_{Twind} \quad (34)$$

$$M = M_{Tmax\ wave} + M_{Twind} \quad (35)$$

6. PRE-DESIGN OF A MONOPILE WIND TURBINE IN THE ROMANIAN SECTOR OF THE BLACK SEA

6.1 Environmental and turbine data

In our work, we consider a wind farm that will be installed in the Romanian sector of the Black Sea approximately 40 km from the coast. We chose the monopile foundation because it has a simple construction and is the most used in offshore areas where the water depth is below 50 m (as in the case of the wind farm site). Therefore, based on the characteristics of the wind and waves of the Black Sea we will evaluate the waves and wind loads on the monopile.

In recent years, several studies have been carried out about the wind and wave climate of the Black Sea[13][14]. These studies provide several data about the wind and waves characteristics like significant wave height, H_s , the significant waves period, T_s , the wind velocity at 10 m above the sea level, U_{10} , and the speed wind standard deviation in different areas of the Black Sea.

In fig.4 are marked the measurement points for the parameters mentioned above, located in the Romanian sector of the Black Sea[14] (points 6, 7, and 8).

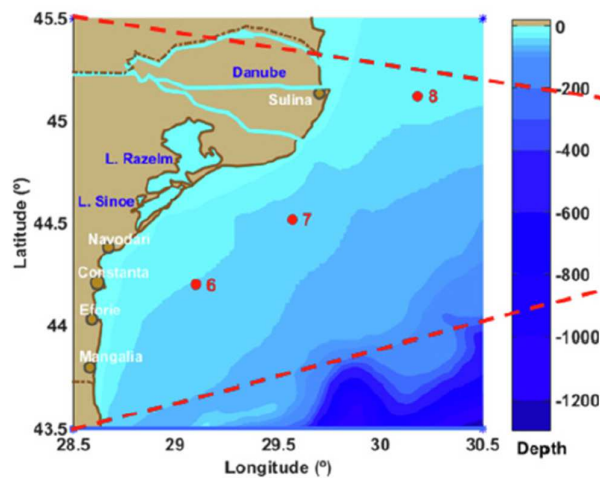


Fig.4. Bathymetry of the Romanian sector of the Black Sea and the locations of points 6, 7, and 8[14].

On the west of the Black Sea, wave and wind climates evaluated between 1987 and 2016 show higher values for wind speed than on the eastern side [14]. Therefore, this area was identified as the optimal condition to install a wind farm[13][14].

Table 1 shows the data regarding water depth, height and period of wave, wind speed, and standard deviation of wind speed [14] at the locations of points 6, 7, and 8 from fig.4.

Table 1
Mean and maximal values for parameters of the waves and wind at the locations of points 6, 7, and 8.

Measurements points	M.U.	6	7	8	Mean values
Water depth, d	m	41	46	35	40.67
Mean H_s	m	0.88	0.89	0.90	0.89
Max H_s	m	7.06	7.10	6.94	7.03
H_{max}	m	12.93	13.04	12.73	12.90
T_{max}	s	12.74	12.80	12.64	12.73
Mean T_s	s	4.54	4.62	4.44	4.53
Max T_s	s	13.19	12.64	12.89	12.91
Mean U_{10}	m/s	6.34	6.38	6.49	6.40
Max U_{10}	m/s	24.75	24.39	24.02	24.39
Mean U_{90}	m/s	7.63	7.68	7.81	7.71
Max U_{90}	m/s	29.78	29.34	28.90	29.34
Standard deviation, U_{10}	m/s	3.01	2.96	3.04	3.00

The salinity of Black Sea water in the superior strata is 17g/l [9]and the density calculated with the relation of Millero and Poisson[10] is 1013 kg/m³ at a temperature of 15°C.

On the basis of the significant height of the wave which is given for a 3-hour period, the maximum height of waves, H_{max} is determined as follows[20]:

$$H_{max} = H_s \sqrt{0.5 \ln(N)} \quad (36)$$

Where N is the number of waves in a period of 3 hours, $N = \frac{10800}{T_s}$.

The period, T_{max} , corresponding to the maximum height of waves is:

$$T_{max} = 11.1 \sqrt{\frac{H_{max}}{g}} \quad (37)$$

The values of H_{max} and T_{max} are shown in table 1.

In the reference [15] we found the average bearing capacity of the marine soil in the west of the Black Sea varies between 198 kPa and 298 kPa(North Romanian coast) and 170kPa to 343 kPa (South Romanian coast). In the calculus, we consider a mean value of 252.25kPa=0.252MPa. Based on this value, $q_{ad} = 0.252$ MPa we can calculate the subgrade reaction coefficient, n_h as follows[2]:

$$n_h = 40q_{ad} = 40 \cdot 0.252 = 10.09\text{MPa/m}^3$$

We consider a turbine of 5MW [26] which has the main characteristics shown in table 2.

Table 2

Wind turbine characteristics.

Turbine parameters	M.U.	Areva M5000-116
Turbine capacity	MW	5
Hub height	m	90
Rotor diameter	m	116
Swept area	m ²	10569
Specific area	m ² /kW	2.12
Number of blades	-	3
Nacelle	tons	246
Tower	tons	350
Rotor and hub	tons	110
Min.rotor speed	rd/min	5.9
Max.rotor speed	rd/min	14.8
Cut-in wind speed	m/s	4
Rated wind speed	m/s	12.5
Cut-off wind speed	m/s	25

6.2 Pre-design of the monopile

The pre-design of the monopile consists in determining the driving length, the diameter, and the wall thickness.

The driving length, L_D of the monopile can be estimated with different methods. In our work we use the Negro et al method [11] and Poulos and Davis method[12]. The first method is based on statistical analysis. In this case, the driven length, L_D depends on the monopile diameter as follows:

$$L_D = 8D - 5 \quad (38)$$

The Poulos and Davis method[12] take into account the subgrade reaction coefficient, n_h of

the soil, and the pile bending stiffness, $E_p I_p$ to determine the driven length. In this case, the driven length, L_D is determined by the following relation:

$$L_D > 4 \left(\frac{E_p I_p}{n_h} \right)^{0.2} \quad (39)$$

If the inequality above is satisfied, the pile is considered slender.

The pile is considered rigid; if the following inequality is satisfied:

$$L_D < 2 \left(\frac{E_p I_p}{n_h} \right)^{0.2} \quad (40)$$

where E_p is the Young modulus of the pile, N/m² and I_p is the second moment of inertia of monopile, in m⁴, determined with the following relation:

$$I_p = \frac{\pi}{4} \left[\frac{D^4}{16} - \left(\frac{D}{2} - t \right)^4 \right] \quad (41)$$

The wall thickness, t , in mm, can be estimated with the API[23] relation:

$$t = 6.35 + D/100 \quad (42)$$

where the monopile diameter, D is in mm.

Array et al.[1] recommended that the total diameter of the substructure, D_s be taken into account when calculating the wave loads. This diameter is determined by the following relation:

$$D_s = D + 2(t_G + t_{TP}) \quad (43)$$

where, D is monopile diameter,m;

t_G – grout thickness between monopile and transition piece, m;

t_{TP} – transition piece wall thickness, m;

Array et al.[1] suggest in their example to take the sum of $t_G + t_{TP} = 0.15$ m.

In our study, we consider that the monopile diameter varies between 3 m and 10 m. Based on these values of diameter, we calculate the substructure diameter, D_s (equation(43)), the wall thickness, t , (equation(42)), and the driven length of the monopile, L_D , with the methods of Poulos and Davies[12], respectively Negro et al.[11] (equation (38) and(39)). The results of calculus are shown in table 3.

Table 3
Monopile diameter, substructure diameter, and driven length.

D	D _s	t	L _D , Poulos Davis[12]	L _D , Negro et al[11]
m	m	m	m	m
3	3.3	0.036	24	19
4	4.3	0.046	30	27
5	5.3	0.056	35	35
6	6.3	0.066	41	43
7	7.3	0.076	46	51
8	8.3	0.086	51	59
9	9.3	0.096	56	67
10	10.3	0.106	61	75

From Table 3 it follows that the method of Negro et al.[11] used to calculate the driven length leads to higher values than the method of Poulos and Davis[12] for diameters greater than 5 m. The differences between the results of the two methods are more accentuated with the increase of the monopile diameter. We consider that the results of the Poulos and Davis method[12] are more confident because this method is based on the parameters of the soil and monopile material compared to the method of Negro et al[11] which is based on the statistics. The monopile wind turbine configuration is shown in fig.5.

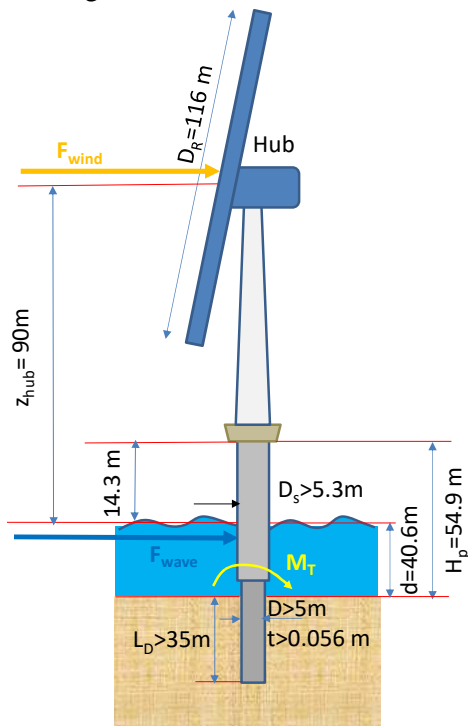


Fig.5. Pre-designed monopile wind turbine configuration.

The height of the platform, measured from the mudline, is determined by the relation [1]:

$$H_p = d + H_{max} + 0.2H_s \quad (44)$$

If we consider $H_{max} = 12.9\text{ m}$, $H_s = 7.03\text{m}$, and $d = 40.6\text{m}$, then the $H_p = 54.9\text{m}$. Therefore, the gap between the mean water level and the platform is $54.9 - 40.6 = 14.3\text{ m}$ which is more than the highest height of the waves (see table 1).

7. RESULTS AND DISCUSSION

To study the wave and wind forces and the bending moments which act on the monopile we consider different working scenarios shown in table 4.

Table 4

Parameters of working scenarios for waves.

Working Scenario	T	H	D _s
	s	m	m
1	12.73	12.90	6.3
2	12.91	7.03	6.3
3	4.53	0.89	6.3
4	12.73	12.90	8.3
5	12.91	7.03	8.3
6	4.53	0.89	8.3
7	12.73	12.90	10.3
8	12.91	7.03	10.3
9	4.53	0.89	10.3

For each working scenario, we calculate the inertia, drag, and total force and also the bending moments with equations (14), (15), (19) to (22).

In the case of the worst scenarios (1st, 4th, and 7th) we compare the results for the total wave forces and total bending moments in the case of using the methods of Vugts et al.[18] and Arany et al.[1] (equations(12) to (15), (17) to(22)). The results of this calculus are shown in tables 5 to 8 and figs.6 and 7.

Table 5

Inertia, drag and total wave forces (Vugts et al.[18] method) for T= 12.73 s and H=12,9 m

D	F _I max,	F _D max,	(F _I /F _D)max	F _T max
in	MN	MN	-	MN
6.3	3.339	1.027	3.249	4.366
8.3	5.796	1.354	4.280	7.149
10.3	8.925	1.680	5.311	10.606

Table 6
Inertia, drag, and total bending wave moments (Vugts et al. method [18]) for T= 12.73 s and H=12.9 m.

D in	M _I max, MNm	M _D max, MNm	(M _I /M _D) _{max} -	M _T max MNm
6.3	75.160	25.403	2.959	100.563
8.3	130.456	33.467	3.898	163.923
10.3	200.901	41.531	4.837	242.432

Table 7
Inertia, drag, and total wave forces for each working scenario (Arany et al. method[1]).

Work. Scen.	F _I max	F _D max	(F _I /F _D) _{max}	F _T max
	MN	MN	-	MN
1	3.339	1.416	2.358	4.754
2	1.804	0.365	4.940	2.169
3	0.275	0.004	67.893	0.279
4	5.796	1.865	3.107	7.661
5	3.131	0.481	6.509	3.612
6	0.478	0.005	0.057	0.483
7	8.925	2.314	3.856	11.239
8	4.822	0.597	8.078	5.419
9	0.736	0.007	110.999	0.743

Table 8
Inertia, drag, and total bending wave moments for each working scenario(Arany et al[1] metod).

Work. Scen.	M _I max	M _D max	(M _I /M _D) _{max}	M _T max
	MNm	MNm	-	MNm
1	111.71	64.77	1.73	176.48
2	50.35	14.81	3.40	65.17
3	10.84	0.13	83.32	10.97
4	193.90	85.33	2.27	279.23
5	87.40	19.52	4.48	106.92
6	18.81	0.17	109.78	18.98
7	298.61	105.89	2.82	404.50
8	134.60	24.22	5.56	158.82
9	28.97	0.21	136.23	29.18

From tables 5 to 8 we observe that the maximum inertia force determined with the two methods (Vugts et al[18] and Arany et al.[1]) has the same values because this has the maximum at the mean water level (zero amplitude) which coincide with the Vugts et al[18] integration limits.

Alternatively, the estimation of the maximum drag force is different when using the two methods. However, the maximum drag force estimated with the method of Vugts et al.[18] is lower than that resulted from applying the equations of Arany et al.[1] because the upper limit of integration in the last case is $\eta = a$. Therefore, when we calculate the maximum total

forces, there is a difference between the calculation results of the two methods. This difference increases slightly with the substructure diameter(fig.6) in our case because the inertia force is dominant and the drag force can be neglected. The larger difference is recorded in the case of the calculation of the total bending moment (fig.7) due to the different integration limits taken into account by the two methods.

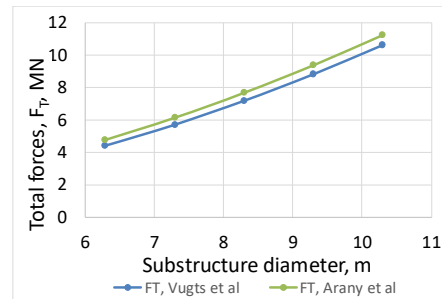


Fig.6. Variation of the total force with the substructure diameter for H=12.9m and T=12.73s.

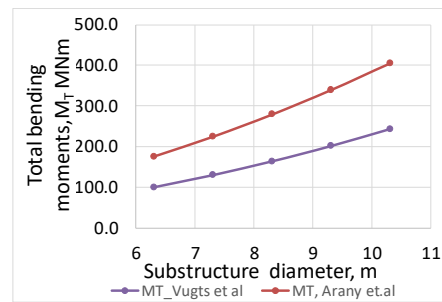


Fig.7. Variation of the total bending moment with the substructure diameter for H=12.9m and T=12.73s.

In the case of the 3rd, 6th, and 9th working scenarios, the equations of Arany et al.[1] lead to huge values of drag moments which is contradictory with the small values of the drag forces. Therefore, the drag moments were determined in these cases with Vugts et al[18] method. In all studied cases, the inertia force was dominant. Also, for most of the working scenarios, the conditions for intermediate water depth were checked, except for working scenarios 3, 6, and 9 which correspond to deep water.

As we see from tables 5 and 6, the maximum values of the bending moment and total forces of waves occurred for the 7th working scenario with substructure diameter D_s=10.3 m, T= 12.73 s, and H=12.9 m. Also, in the case of the 3rd

working scenario ($D_s=6.3$ m, $T= 4.53$ s, and $H=0.89$ m), the total force, respectively the total bending moment are the smallest. In the case of the first extreme scenario (the highest period and height of wave), we plot the variation of the wave forces with time and the maximum values of these forces with the substructure diameter. Also, we plot the variation of the maximum bending moments with the substructure diameter (fig. 8 to 10).

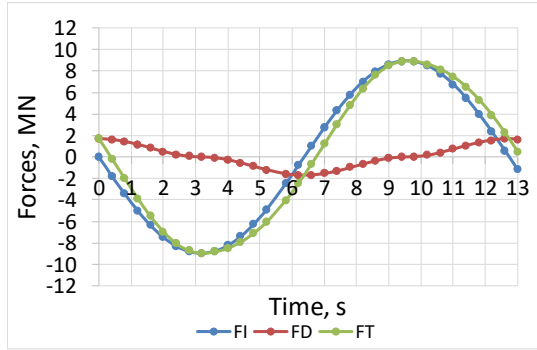


Fig.8. Variation of the inertia, drag, and total force with the time for substructure diameter of 10.3m, $H=12.9$ m, and $T=12.73$ s

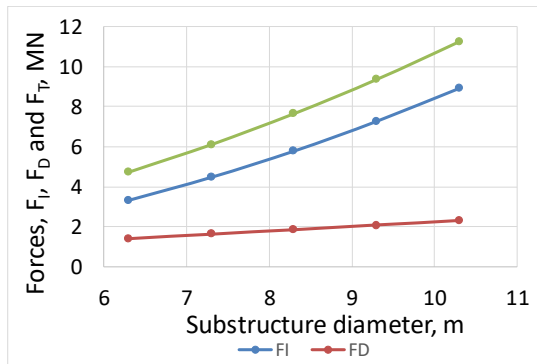


Fig. 9. Variation of total force with the substructure diameter, for $T=12.73$ s and $H=12.9$ m (method of Array et al [1]).

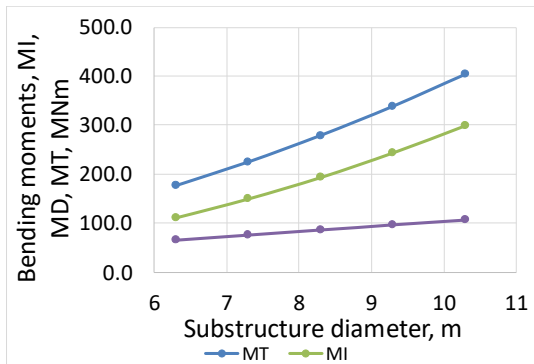


Fig.10. Variation of the inertia, drag, and total bending moments with the substructure diameter for $T=12.73$ s and $H=12.9$ m.

Table 1 shows, also, the available data for wind as mean and maximum wind speed which correspond to the mean wave height and period and maximum wave height and period and standard deviation of wind speed at 10 m above the mean sea level.

For the two values of wind speed, we calculated the total wind load and the total bending moment (relation (24) to (33)). The results of calculus are shown in table 9.

Table 9

Wind load and total bending moment.

U	u_{ext}	$\sigma_{U,c}$	F_{wind}	M_{windT}
m/s	m/s	m/s	MN	MNm
7.71	5.190	2.007	1.133	200.047

Once the total wave force and wind force, as well as the total wave bending moment and the wind bending moment we can determine the total force and the total bending moment (relation (34) and (35) for all the monopile diameter scenarios considered. The results of calculus are shown in table 10.

To estimate the minimum value of the monopile diameter according to the references [1][20] we will check the following relation:

$$\sigma_m < \frac{\sigma_c}{\gamma_M} \tag{45}$$

where, σ_c and σ_m are yield strength in MPa, respectively maximum stress and γ_M is a material factor.

The maximum stress is determined by the following relation [1][20]:

$$\sigma_m = \frac{M_{Tmax}D}{2I_p} \tag{46}$$

where the material factor $\gamma_M = 1.1$, σ_c is yield strength in MPa.

In our study, we consider S355 steel (the most used for monopile) with minimum yield strength

$\sigma_c = 355$ MPa and Young modulus $E=210$ GPa.

Therefore, $\sigma_m < 322.72$ MN/m².

Using, the relation (46) we calculate the maximum stress given by the lateral loads (wind and wave) for different values of monopile diameter. The results of this calculus are shown in table 10.

Table 10
Total load, total moment and maximum stress

D_s	I_p	F_T	M_T	σ_m
m	m^4	MN	MNm	MPa
4.3	1.488	3.654	296.298	428.119
5.3	3.353	4.687	333.599	263.656
6.3	6.853	5.887	376.531	173.073
7.3	11.725	7.256	425.09	132.331
8.3	19.412	8.794	479.28	102.463
9.3	30.371	10.499	539.099	82.540
10.3	45.422	12.372	604.547	68.544

From table 10 it is evident that the minimum diameter for the monopile is 5m, respectively 5.3 m for the substructure diameter.

For a rigorous design of a monopile wind turbine, it is necessary to have much more data regarding the wave, wind, and marine soil characteristics and also the specialized software.

8. CONCLUSION

A wind farm installed in the Romanian sector of the Black Sea is a huge opportunity in the actual context of promoting renewable energy.

Therefore, a pre-design of a monopile offshore wind turbine with minimum available data is important to assess the preliminary dimensions of a wind farm and also the gross costs.

Based on the minimum data regarding the characteristics of wind and waves from the Romanian Sector of the Black Sea, we calculated the total forces and bending moments generated by the waves and wind in the case of different working scenarios and with two methods. The differences between the two methods are the integration limits which lead to different results in the calculus of the maximum drag force and maximum bending moment determined by the drag force.

In all the cases studied, the inertia force was dominant. Also, in most working scenarios, the condition of the intermediate water was checked.

We identify the worst scenario with the biggest forces and bending moments. Alternatively, we found that these forces and moments increase with the diameter of the monopile. Based on the mean bearing capacity of the marine soil we determined the driven

length for several values of the monopile diameter.

Further, using the criterion that maximum stress does not exceed the yield strength of the monopile material we selected the minimum diameter of the substructure and the corresponding driven length of the monopile. Therefore, we determined the principal dimensions of a wind turbine monopile that will be installed in the Romanian Sector of the Black Sea.

We mention that we considered only the wind and wave loads because these are the most important in a pre-design phase. In the case of the final design, it is necessary to consider all the loads and much more environmental data.

9. REFERENCES

- [1] Arany, L., Bhattacharya, S., Macdonald, J., Hogan, J., *Design of monopiles for offshore wind turbines in 10 steps*. Journal of Soil Dynamics and Earthquake Engineering, Vol.92, pp.126–152, 2017.
- [2] Bowles J. E., *Foundation Analysis and Design*. 5th edition New York: McGraw-Hill, 1996.
- [3] Chakrabarti, S., *Handbook of offshore engineering*, Vol.1, Elsevier, Amsterdam, 2005.
- [4] Chen, J., Kim, Moo-Hyun., *Review of recent offshore wind turbine research optimization methodology in their design*. Journal of Marine Science and Engineering, Vol. 10, pp.2-28, 2022.
- [5] Frohboese P, Schmuck C., *Thrust coefficients used for estimation of wake effects for fatigue load calculation*. European Wind Energy Conference Warsaw, Poland, pp 1–10, 2010.
- [6] Gupta, B., Basu, D., *Offshore wind turbine monopile foundations: Design perspectives*. Ocean Engineering, Vol.213, 107514, pp.1-17, 2020.
- [7] Hau, E., *Wind Turbines: Fundamentals, Technologies, Application, Economics, 2nd edition*, Springer, 2006
- [8] Lee, J, Zhao, F., *Global Wind Report 2022*, Global Wind Energy Council, 2022.

- [9] Mihailov, M.-E., *Dinamica maselor de apa in Nord-Vestul Marii Negre, Ex Ponto*, 2017
- [10] Millero F.J., and Poisson, A., *International one-atmosphere equation of state of seawater*, Deep-Sea Research 28A (6) pp. 625–629, 1981.
- [11] Negro, V., Lopez-Gutierrez, J.-S., Esteban, D., M., Alberdi, P., Imaz, M., Serracilara, J.-M., *Monopiles in offshore wind: Preliminary estimate of main dimensions*, Ocean Engineering, Vol.133, pp.253-261, 2017.
- [12] Poulos H, Davis, E., *Pile foundation analysis and design*. Rainbow-Bridge Book Co, 1980
- [13] Rusu, L., Ganea, D., Mereuta, E., *A joint evaluation of wave and wind energy resources in the Black Sea based on 20-year hindcast information*, Energy Exploration & Exploitation, Vol.36(2) pp.335-351, 2018
- [14] Rusu, L., *The wave and wind power potential in the western Black Sea*, Renewable Energy, 139, pp.1146-1158, 2019.
- [15] Stanciucu, M., *Actual geological processes acting on the western coast of Black Sea*, SGEM, Albena, Bulgaria, 2014.
- [16] Shu, Z.R., Jesson, M., *Estimation of Weibull parameters for wind energy analysis across UK*, Journal of Renewable and Sustainable Energy 13, 023303, 2021.
- [17] Van der Tempel, J., Diepeveen, N.F.B., Cerda Salzman, D., J., de Vries, W.E., *Design of support structures for offshore wind turbines*, Chapter 17, WIT Transactions on State of the Art in Science and Engineering, Vol 44, WIT Press, 2010.
- [18] Vugts, J. H., van der Tempel, J., Schrama, E. A., *Hydrodynamic loading on monotower support structures for preliminary design*, Technical University Delft, 2001.
- [19] Energy Policy Group, *Romania's offshore wind energy resources. Natural potential, regulatory framework, and development prospects*, Bucharest 2020.
- [20] Det Norske Veritas, *Offshore Standard DNV-OS-J101 Design of Offshore Wind Turbine Structures*. Høvik, Norway, 2014.
- [21] IEC International Standard IEC 61400-3 *Wind turbines - Part 3: Design requirements for offshore wind turbines, 1.0 ed. International*, 2009 Electrotechnical Commission (IEC)
- [22] IEC International Standard IEC-61400-1, *Wind Turbines- Part 1: Design requirements*, third Edition, 2005.
- [23] API, *Recommended practice for planning, designing and constructing fixed offshore platforms—working stress design: API recommended practice 2A-WSD (RP2AWSD)*, Dallas, 2000.
- [24] <https://www.airpes.com/wind-turbine-parts>
- [25] https://en.wikipedia.org/wiki/Wind_turbine
- [26] <https://en.windturbine.com/turbines/23-areva-m5000-116>

Studiu privind predimensionarea unui monopilon ce suporta o turbina eoliana instalat in sectorul romanesc al Mării Neagre

Rezumat. În lucrare se prezinta caracteristicile generale ale unei turbine eoliene instalata in mediul marin si de asemenea un studiu al sarcinilor generate de mediul marin care acționează asupra suportului acesteia. După cum reiese din multe studii publicate în ultimii ani, vestul Mării Negre este potrivit pentru instalarea unui parc eolian eficient. Am ales o substructură monopilon deoarece aceasta este potrivită pentru adâncimea apei din zona respectiva. Pe baza datelor de mediu din sectorul românesc al Mării Negre, s-a studiat modul în care caracteristicile mediului marin și dimensiunile monopilonului influențează forța totală și momentul total care acționează asupra structurii. În acest fel, am identificat cel mai dificil scenariu și am analizat dimensiunile monopilonului pentru a propune o predimensionare a acestuia.

MARCU Mariea, Associate Professor, Ph.D. Eng. Petroleum and Gas University of Ploiesti, Department of Well Drilling, Extraction and Transport of Hydrocarbons, Email: mmarcu@upg-ploiesti.ro, + 40 - 244.573 171